Surface Review and Letters, 2550175 (18 pages)

DOI: 10.1142/S0218625X25501756

World Scientific
www.worldscientific.com

MACHINE LEARNING-BASED PREDICTION OF SURFACE CHARACTERISTICS AND TOOL WEAR IN Mg–AZ91D MILLING UNDER DISTINCT CONDITIONS

Z. A. AMJATH[*,§], R. GANESA MOORTHY[†], K. S. ASHRAFF ALI[*] and C. GNANAVEL[‡]

[*]*Department of Mechanical Engineering, C. Abdul Hakeem College of Engineering & Technology, Ranipet, Tamil Nadu, India*

[†]*Department of Mechanical Engineering, Chennai Institute of Technology, Kundrathur, Chennai, Tamil Nadu, India*

[‡]*Department of Mechanical Engineering, Vels Institute of Science, Technology and Advanced Studies, Pallavaram, Chennai, Tamil Nadu, India*

[§]*zaamjath28@gmail.com*

Received 3 June 2024
Revised 12 September 2024
Accepted 20 April 2025
Published 4 June 2025

As industries seek greener alternatives to mineral oil-based cutting fluids due to their negative environmental impact, vegetable oils emerge as promising substitutes. Their biodegradable and nontoxic properties make them particularly suitable for machining operations. This study investigates the impact of different lubrication and cooling (L/C) methods on machined surfaces and machining parameters to develop sustainable milling practices for Mg-AZ91D. Effective L/C is crucial in regulating heat and friction to enhance product quality. Experimental milling trials involving dry, minimum quantity lubrication (MQL), and solid lubricant (SL) with MQL were conducted on Mg-AZ91D. Results show that under SL-MQL conditions, surface roughness (Ra) was significantly lower (by 49–70%) compared to dry conditions and marginally lower (by 8–13%) than with MQL alone. Additionally, machine learning (ML) algorithms were employed for predictive modeling, including linear regression (LR), support vector machine (SVM), and Random Forest (RF). These models were compared using performance metrics such as R^2, MAE, RMSE, RAE, and RRSE. The RF algorithm demonstrated the best results in predicting surface characteristics, exhibiting notably higher R^2 scores and performance metrics. Conversely, SVM outperformed other algorithms in predicting tool wear. The ML models revealed that cooling conditions had a greater impact on output milling parameters compared to other input variables.

Keywords: Mg-AZ91D; solid lubricant; machine learning; random forest; SVM.

[§]Corresponding author.

1. Introduction

Due to their strength and outstanding density, Mg-AZ91D is frequently employed in cutting-edge applications. Some examples of these applications include the aviation industry and the medical implant sector. When it comes to orthopedic implants, biodegradable Mg-AZ91D is typically and widely preferred over steel, titanium, and cobalt-based alloys. This is because biodegradable Mg-AZ91D can reduce costs and weight while also preventing undesirable outcomes such as metal ion release and stress shielding.[1] Mg and the alloys it may form have a high degree of machinability, which makes dry machining a viable alternative. Despite this, previous research has uncovered a variety of potential hazards associated with machining Mg-AZ91D, including the possibility of self-ignition as well as a strong reaction between Mg and oxygen that results in the production of hydrogen gas. These hazards are especially prevalent in applications that involve water-based coolants and dry cutting, respectively. It was discovered that the magnitude of the −Mg17Al12 state in the Mg structure influences the ease of self-burning, which ultimately leads to chip burning.[2] Dry milling of Mg-alloys is an economical and ecologically responsive cutting technology that is broadly employed in industrial production. Coating-equipped tools could be employed to lower adhesion and friction in the tool-workpiece (W/p) contact, leading to lower machining forces and better surface conditions.[3] Even though dry machining doesn't require the use of any kind of cutting oil (CO), it is not a sustainable process since it results in increased surface roughness (Ra) and tool wear, which in turn leads to lower product quality and productivity.[4] Several examinations were previously conducted to resolve hitches in the cutting of Mg-AZ91D.

Choosing a C/L technique is a crucial aspect of machining Mg-AZ91D. Previous research has looked into many options, including minimum quantity lubrication (MQL), dry machining, and cryogenic cooling.[5] Amid these approaches, the MQL system has proved to be a decent substitute, for instance. MQL is a novel C/L approach. Using pressured air, tiny oil droplets are precisely directed into the area where the cutter and W/p contact. The main advantage of MQL over conventional cooling strategies is its much lower CO usage, usually about 50 ml/h.[6] Li *et al.*[7] studied the wear process and failure patterns of uncoated, TiAlN-coated, edge-strengthened, and diamond-coated cutters in the milling of rare-earth (RE) Mg-AZ91D with MQL and dry conditions. A cutter wear lessening of 55% was attained by the MQL for the unstrengthened tool.[7] Xu *et al.*[8] examined the influence of distinct cutting settings on the cutting performance of GW63K Mg–RE alloy. To accomplish this, several experiments were conducted, which included both no-coolant and MQL conditions. MQL was presented to be capable of lowering milling temperatures by 10.8% on average in relation to the dry strategy.[8] Due to their biodegradability and non-toxicity, vegetable oils (VO) are becoming attractive MQL cutting lubricants.[9] The lubricants from castor oil and sunflower minimize friction and tool wear during metal cutting. MQL systems use VO to improve surface quality and tool life over dry machining and flood cooling.[10] Using a VO in MQL system, Alshibi *et al.*[2] evaluated and improved the machinability (high-speed) of AZ91 by employing grey relational analysis (GRA) based on tool wear and chip morphology. With a 20% contribution for the GRA grade, the MQL flow was considered as the essential variable.[2] Even though MQL has more advantages, its limited cooling capacity can be insufficient for effectively dissipating heat in high-speed machining operations.[11] Because of its capacity to significantly improve fluid performance by regulating heat and lessening friction amid the cutter and the W/p, the solid lubricant (SL)-assisted MQL approach is gaining increased recognition. This is because it can do all this while avoiding the significant costs and complications associated with cryogenic temperatures, which are often required in hybrid techniques.[12] Makhesana and Patel[13] examined the capabilities of MQL and SL in the context of the machining process. Calcium fluoride (CaF_2) SL powder particles measuring microns in size were combined with SAE 40 CO and then supplied to the cutting area using MQL. Manufacturing that is both clean and sustainable may be achieved through the usage of MQL with SL.[13]

The literature claims that cooling conditions and input parameters affect the surface trait of the parts. Current studies have shown that the adoption of online monitoring tools, such as acoustic emission sensors and machine vision systems, may increase productivity and tool life.[14] Online monitoring

systems and ML techniques are being increasingly integrated to forecast ideal machining parameters and defect finding as a predictive maintenance key. ML approaches are highly beneficial in enhancing the forecasting of many areas, including tool wear, cutting forces, tool life, and Ra prediction.[15] Using RF and GPR ML algorithms, Motta *et al.*[16] developed models for the prediction of W/p Ra in cylindrical turning operations. The Root Mean Square Error (RMSE) predictions of the proposed models were assessed. According to the experimental findings, GPR outperforms RF for training sets that comprise 67–90% of the dataset in terms of consistency and quality.[16] Using real production data, Brillinger *et al.*[17] applied several ML methods, particularly versions of the decision tree (Decision Tree, RF, and boosted RF), to estimate the energy ingesting of CNC machining processes. The RF approach yields the best accurate energy demand forecasts.[17]

Although previous research has shown that ML can improve predictions for a few aspects of different machining processes, its ability to optimize C/L methods for Mg-AZ91D machining remains unexplored. Incorporating ML algorithms to model and anticipate milling performance under distinct environmental conditions is a novel way to optimize Mg-AZ91D machining for sustainability, enhanced productivity, and tool life. To date, significant research has been focused on the cutting of Mg-AZ91D, the supply of MQL, and the properties of tool coatings. However, no research has been found on the forecasting of milling parameters with distinct environmental (dry, MQL, and MQL-SL) conditions for Mg-AZ91D using ML. As a result, the purpose of this research is to investigate how ML algorithms may be used to establish a correlation among the variables of milling Mg-AZ91D. The ML algorithms chosen for this research are RF, SVM), and LR.

2. Materials and Methods

2.1. *Workpiece and conditions*

A flat plate of AZ91D Mg alloy, with a dimension of 20*20*1 cm was chosen for the experimental study. The YCM milling machine is used for this study, which is presented in Fig. 1. The chemical elements of W/p are outlined in Table 1. The experiments were structured based on a variety of factors and their

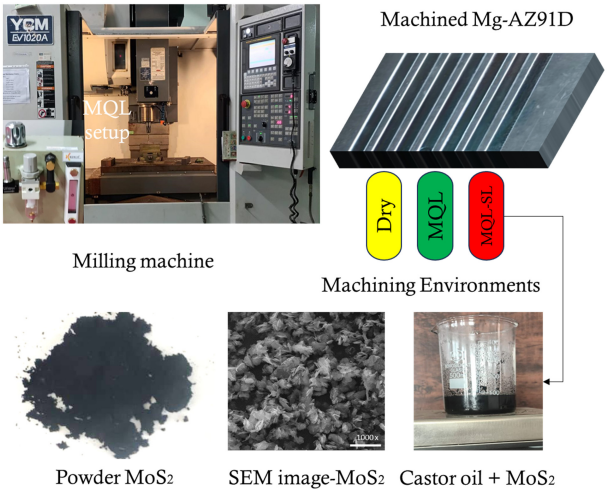

Fig. 1. (Color online) Presentation of experimental work.

Table 1. Chemical elements of Mg-AZ91D.

Al	Mn	Zn	Si	Cu	Ni	Fe	Mg
8.5	0.20	0.55	0.10	0.03	0.002	0.005	Bal.

corresponding levels. A total of 18 experiments were carried out, with each set of conditions comprising six experiments. In the initial set of tests, cutting parameters were adjusted within a dry environment. The subsequent series of experiments involved the implementation of MQL and SL-MQL. In SL-MQL, solid MoS_2 lubricant is incorporated with castor oil (CaO). To ensure a consistent supply of SL-MQL, the nozzle was positioned at a fixed 45° angle counterclockwise to the rotation direction of the drill tool. The particulars of experimental work are presented in Table 2.

2.2. *Measurement methods*

In this research study, surface roughness and wear characteristics were meticulously investigated using

Table 2. Details of experimental work.

Machining type	Milling
Machine model	YCM-EV1020A
Insert model and coating	1135PDER, PVD-TiAlN
Nose radius	0.8 mm
No. of flutes	1
MQL oil	CaO
MQL flow rate	70 ml/h
Air pressure in MQL	4 bar

advanced instrumentation. The SE-2500 surface roughness tester was employed to acquire precise measurements of surface roughness, providing valuable insights into the texture and finish of the machined surfaces. The Talysurf system was utilized for the detailed examination of three-dimensional topography, enabling a comprehensive understanding of surface features and irregularities. The VMS 2100 played a crucial role in measuring flank wear, offering quantitative data on tool degradation and wear patterns during machining processes. Additionally, scanning electron microscopy (SEM) images were captured using JEOL equipment, providing high-resolution visualizations to scrutinize the microstructural changes and wear mechanisms in the machined specimens.

3. Environmental Conditions

The schematic presentation of the different environmental conditions is displayed in Fig. 2. Dry Machining: In the initial phase of the experiments, the milling process was carried out in a dry setting, devoid of any external lubricants or coolants. This approach enabled an evaluation of the baseline performance and thermal dynamics of the AZ91D magnesium alloy in the absence of external influences.

MQL: Following the dry machining tests, MQL cooling condition is introduced. MQL involves a minimal amount of lubricant, often in the form of a mist or aerosol, into the cutting zone. This controlled lubrication serves to mitigate friction and heat generation during machining, enhancing tool longevity, and surface finish. Importantly, MQL is chosen for its environmental benefits, offering a reduced ecological footprint compared to conventional flood cooling systems.

SL-MQL: Under the SL-MQL condition, solid MoS_2 lubricant was integrated into the lubrication system. MoS_2, renowned for its low friction and anti-wear characteristics, constituted 20% of the SL weight blended with CaO. In the study by Velmurugan *et al.*,[18] the same percentage of SL was taken. It was determined that the most effective range for MoS_2 particle size fell within the concentrations ranging from 10 microns to 15 microns. Using more than 20% MoS_2 content had the potential to cause nozzle tip blockage due to its high viscosity. This approach aimed to optimize lubrication efficacy while steering away from nozzle blockage issues associated with higher concentrations of MoS_2. The incorporation of SL within MQL aligns with sustainability goals by minimizing reliance on liquid coolants, rendering the machining process more eco-friendly. The diverse environmental conditions were meticulously chosen to scrutinize the influence of lubrication methods on the milling dynamics of Mg-AZ91D.

4. Results and Discussion

4.1. *Effect of surface roughness*

When machining Mg-AZ91D, the choice of cutting environment is crucial to ensure efficient and safe operations. Mg-AZ91D is known for its flammability and susceptibility to ignition, making proper environmental control essential.[19] There are several cutting environments commonly employed when working with Mg. Figure 2 presents the interaction of the tool and work W/p with distinct environmental conditions. Figure 3 presents the disparity in Ra under diverse speed-feed combinations. The Ra achieved under SL-MQL conditions is 8–13% lower than that obtained under MQL cutting technique and 49–70% lower than that obtained under dry

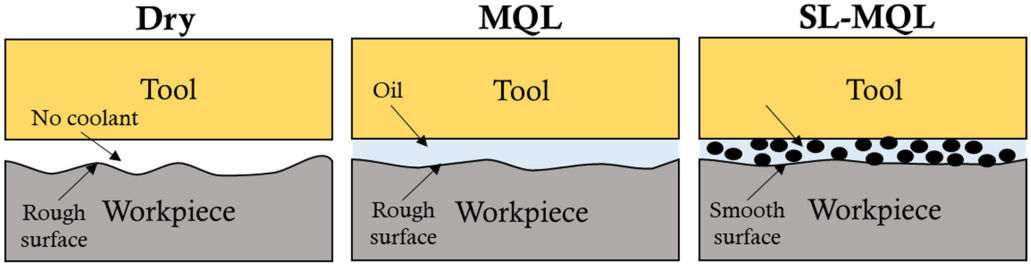

Fig. 2. (Color online) Schematic of tool and W/p interaction with distinct environmental conditions.

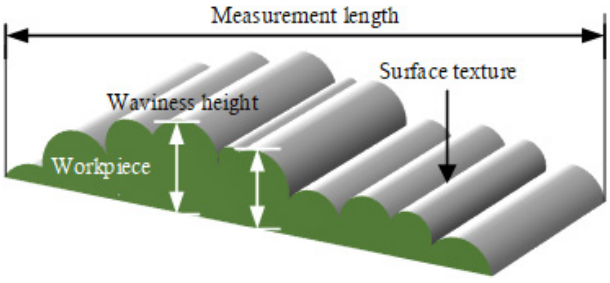

Fig. 3. (Color online) Schematic of roughness profile.

conditions. Dry machining of Mg-AZ91D often results in elevated Ra. This is primarily because of the high heat generated during cutting that can cause material adhesion to the tool and irregularities on the machined face. The absence of lubrication and cooling (L/C) makes it challenging to achieve a smooth finish, and tool wear can further contribute to surface imperfections.[20] MQL is a more controlled approach that can significantly improve Ra when machining Mg-AZ91D. Precisely applying a minimal amount of lubricant or coolant in the form of a fine mist, helps in diminishing the heat at the cutting region.[21] This controlled cooling action minimizes the likelihood of adhesion, resulting in a smoother machined surface. MQL also extends tool life, which further contributes to surface finish quality. When MQL is combined with SL like MoS_2, the surface finish quality is enhanced even further. The SL creates a boundary layer that reduces friction and heat, resulting in improved Ra. The synergistic effect of MQL and SL makes this method particularly effective in achieving superior surface finishes on Mg-AZ91D W/ps.[18]

Figure 4 presents the displays of surface topography and SEM images of the machined face. Under dry machining conditions, SEM images revealed prominent scratches and irregular feed marks on the face of the Mg-AZ91D. The nonpresence of lubrication under the dry cutting strategy led to a significant friction between the cutter and W/p, resulting in surface imperfections and roughness.[22] The lack of a cooling medium worsened the tool wear and contributed to the undesirable surface characteristics observed in the SEM images. In the case of MQL, the SEM analysis displayed distinct ploughing patterns on the machined Mg-AZ91D face. While the introduction of minute lubrication reduced friction and improved the cutting process compared to dry conditions, the ploughing effect indicated a moderate level of tool wear and material deformation. The ploughing effect is because of the sliding of the cutting edge over the material rather than slicing it, due to less cooling effect.[23] Remarkably, the implementation of MQL with SL yielded significantly improved results. SEM images exhibited a notably smoother surface with minimal signs of wear and deformation. The presence of the SL effectively reduced friction, preventing excessive tool wear and material displacement. As a result, the Mg-AZ91D surface appeared more refined and freer from the scratches and irregularities observed in the dry and MQL conditions. Additionally, 3D topography (right side) images corroborated the SEM

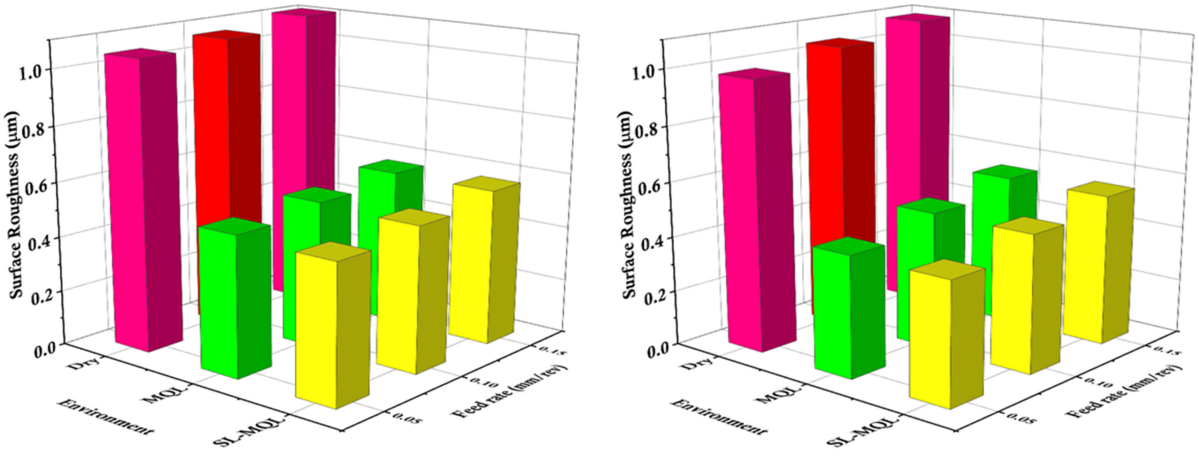

(a) (b)

Fig. 4. (Color online) Effect of coolant (a) Vc = 60 m/min and (b) Vc = 90 m/min.

findings, providing a comprehensive visualization of the surface texture (see Fig. 5). In the no coolant condition, the topography images highlighted the high peaks and valleys, indicating an absence of lubrication and ineffective heat dispersion. In the MQL condition, the surface showed a relatively improved texture. The surface machined with SL-MQL exhibited remarkably fewer peaks and valleys. The SL played a pivotal role in enhancing the lubrication and reducing friction.[24]

4.2. *Effect of flank wear*

When machining Mg-AZ91D, the choice of cutting coolant plays a critical role in defining the extent of flank wear (Vb) on cutting tools.[25] Figure 6 presents the image of a tool with EDS. Figure 7 presents the variation in Vb under distinct speed-feed combinations. The Vb attained under SL-MQL circumstances is 8–11% lower than that under MQL settings and 41–54% lower than that under the dry cutting method. In dry machining, the absence of L/C results in high temperatures and increased friction at the tool-chip interface. These conditions accelerate Vb, leading to reduced tool life and diminished machining precision.[26] Conversely, MQL with CaO provides a more favorable environment. CaO serves as an effective coolant and lubricant, which reduces the heat generated during cutting and minimizes friction. Consequently, Vb is significantly lessened compared to dry machining, resulting in extended tool life, and improved cutting precision.[27] Taking it a step further, the introduction of SL, such as MoS_2, in the MQL environment offers remarkable benefits. MoS_2 forms a defensive boundary layer on the cutters' surface, further decreasing friction and

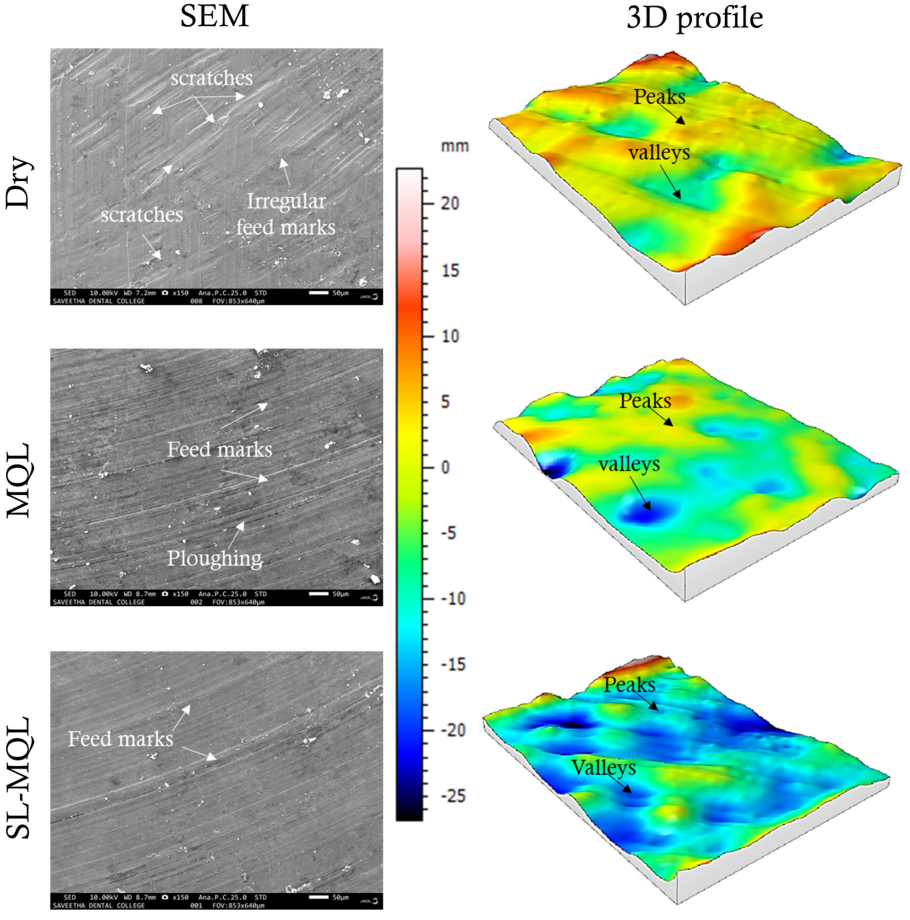

Fig. 5. (Color online) SEM images (left side) and 3D topography (right side) of machined face at a Vc = 90 m/min and $f = 0.15$ mm/rev.

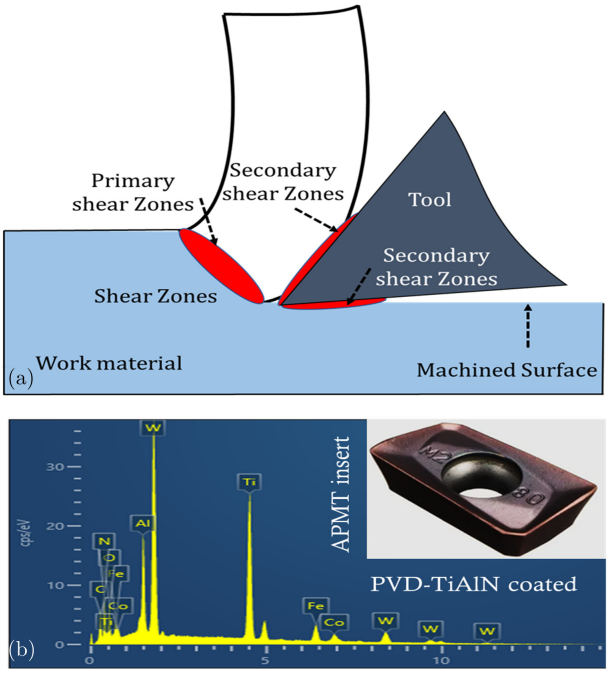

Fig. 6. (Color online) (a) Schematic of shear zones and (b) Coated tool with EDS image.

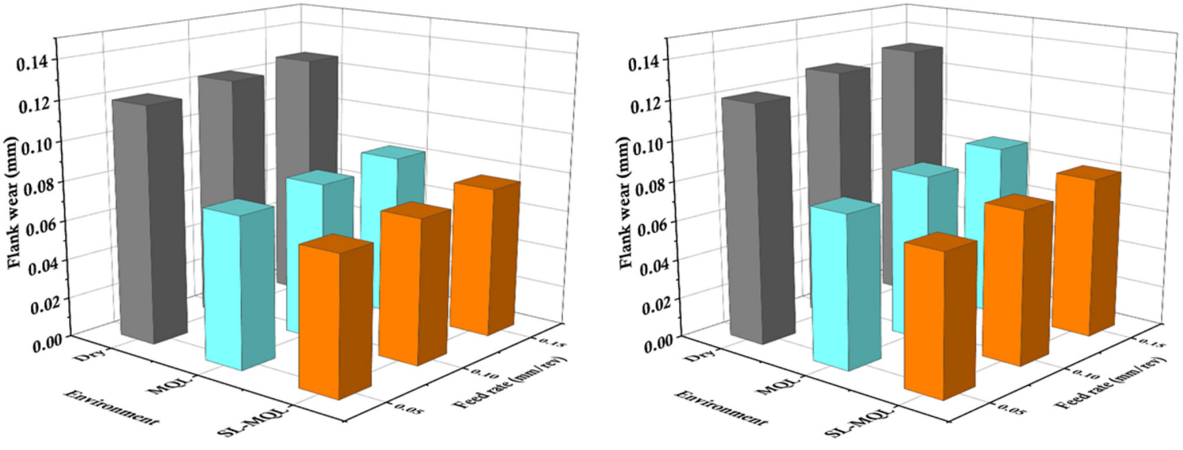

(a) (b)

Fig. 7. (Color online) Effect of coolant (a) Vc = 60 m/min and (b) Vc = 90 m/min.

heat. This leads to a substantial decrease in Vb, ensuring tools remain sharper for longer periods, ultimately improving machining efficiency and surface finish.[28]

SEM images show (Fig. 8) clear visual evidence of the wear mechanisms experienced by cutting tool inserts during the cutting of Mg-AZ91D under diverse cooling conditions. Under dry machining conditions, SEM images revealed a complex array of wear mechanisms on the cutting insert. These included abrasion, attrition, and coating delamination. The absence of L/C in dry conditions led to substantial heat and increased friction between the cutter and W/p. The abrasive wear was evident as material removal from the tool insert, while attrition indicated the gradual breakdown of the tool material. Moreover, coating delamination, the detachment of the defensive coating from the tool surface, further

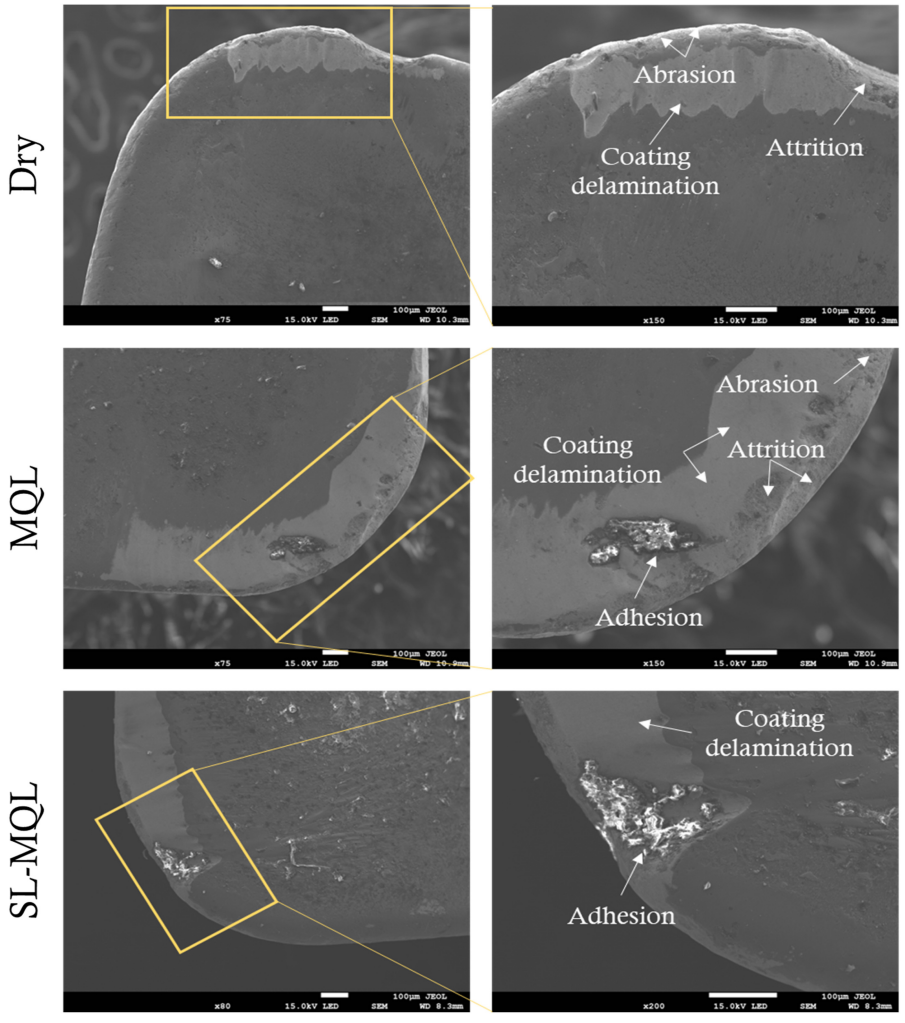

Fig. 8. (Color online) SEM images of tool wear at a Vc = 90 m/min and $f = 0.15$ mm/rev.

exacerbated tool wear, reducing tool life, and effectiveness.[14] In the case of MQL, SEM analysis exhibited a variety of wear patterns on the tool insert. These included abrasion, adhesion, attrition, and coating delamination. While MQL introduced minimal lubrication and reduced friction compared to dry conditions, the combination of high-speed machining and the inherent properties of Mg-AZ91D still subjected the tool to significant wear. Abrasion and attrition were indicative of material loss from the tool, whereas adhesion highlighted the tendency of W/p material to stick to the tool surface.[29] Coating delamination remained an issue, suggesting that MQL alone did not fully mitigate this wear mechanism. Remarkably, the implementation of SL-MQL demonstrated an altered wear pattern on the cutting tool insert. In this case, SEM images primarily showed adhesion and coating delamination. The presence of SL significantly reduced friction and enhanced lubrication, thereby decreasing the abrasive and attrition wear. The notable absence of attrition in the wear patterns was a positive sign of reduced tool wear. Adhesion, however, indicated some material transfer from the Mg-AZ91D to the tool surface. Coating delamination remained, albeit to a lesser extent than in the dry and MQL conditions.

5. Machine Learning Algorithms

ML algorithms are tools that enable computers to learn from data and make forecasts or decisions.[30] They include supervised, unsupervised, and reinforcement learning algorithms, each suited to specific tasks and data types. These algorithms are pivotal in

fields like healthcare, automotive, and manufacturing sectors.[31] In this research work, three distinct ML algorithms were selected and the architectures are presented in Fig. 9.

LR is a fundamental statistical method for modeling the association amid a dependent and one or more independent variables.[32] It seeks to identify the linear equation that provides the best fit, which is frequently shown as $Y = aX + b$, where Y refers to the variable that is being analyzed, X refers to the variable that is being analyzed independently, and a and b are coefficients. The primary objective is to achieve a reduction in the total area under the curve represented by the squared sum of the disparities between the anticipated and actual values. LR is frequently used for tasks including result prediction, variable effect quantification, and trend identification in a variety of domains, including science, economics, and finance.

SVM is a potent ML technique that is applied to regression and classification.[15] In a high-dimensional space, SVM finds the best hyperplane to divide data points into diverse groups. Accelerate the margin — the space amid the hyperplane and the closest data points for each group — is the aim. SVM employs the "kernel trick" to map data into larger-dimensional spaces when it's not linearly separable. SVM excels in high-dimensional spaces, handles nonlinear data through kernel functions, and resists overfitting in small to medium-sized datasets. It's primarily used for binary classification, though it can handle multiclass problems. However, SVM's performance is sensitive to kernel choice and hyperparameter settings, and it may not be ideal for large datasets due to computational complexity.

Robust ensemble ML algorithm RF, is well-suited for applications involving classification and regression.[33] To increase accuracy and dependability, it builds several decision trees and associates their forecasts. Individual decision tree is built using an arbitrary subset of the training data, a method

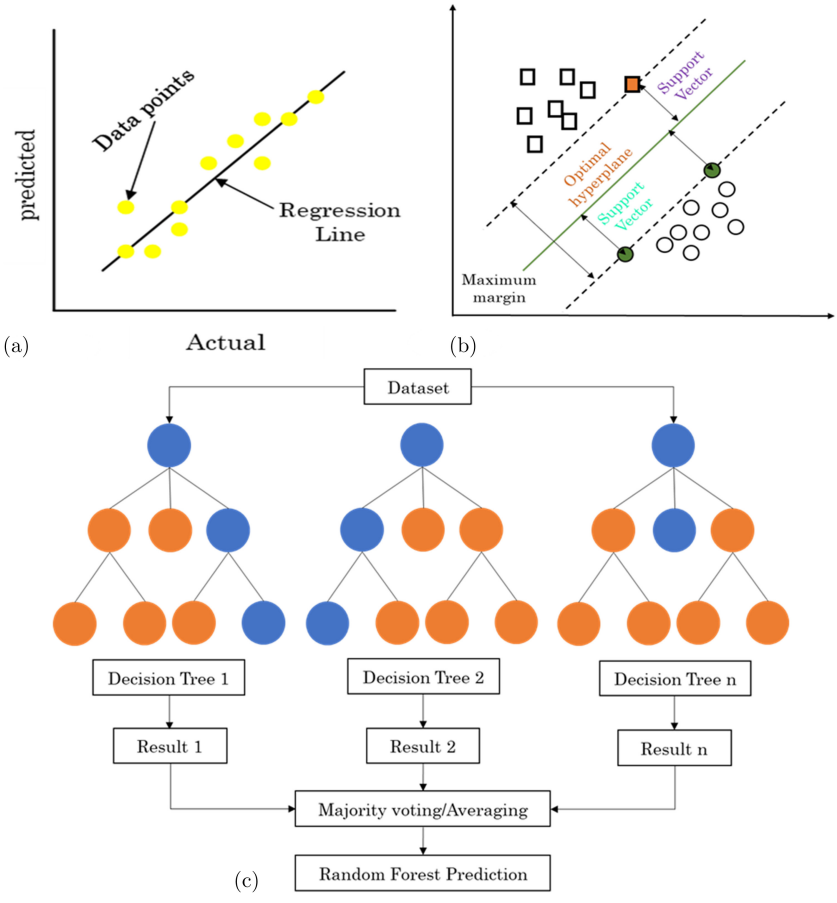

Fig. 9. (Color online) Illustration of (a) LR, (b) SVM, and (c) RF.

acknowledged as bootstrapping, which introduces diversity into the model. Additionally, RF employs feature bagging by considering only a random subset of features at each split in the trees. In making a forecast, it utilizes voting for classification and averaging for regression. RF offers high accuracy and is less susceptible to overfitting in relation to separate decision trees. It can handle missing data and provides insights into feature importance, aiding feature selection, and data analysis. Its versatility and robustness make it a popular choice across various domains, including finance, healthcare, and image classification, where accurate and dependable forecasts are paramount.

6. Forecasts with ML Models

In this study, the predictive power of three distinct ML algorithms LR, SVM, and RF — to model the intricate relationships amid machining parameters and two critical outcomes: Ra and Vb is analyzed. Figures 10 and 11 show the training, cross-validation, and testing of different algorithms for Ra and Vb. To evaluate the predictive performance of these algorithms, we conducted rigorous training, cross-validation, and testing experiments. When predicting Ra, the training phase revealed that LR had a modest performance, with forecast points scattered around the actual values. SVM exhibited improved accuracy, with forecast points clustering more tightly compared to LR. However, it was in the cross-validation and testing phases that the true distinction emerged. SVM consistently demonstrated better predictive performance, producing forecast points that closely matched the actual values. In contrast, RF outperformed the other algorithms, with forecast points displaying exceptional accuracy and minimal scatter. For Vb forecast, LR's training points were widely dispersed, indicating limited precision, while SVM showed better accuracy. Cross-validation and testing phases confirmed SVM's advantage in Vb forecast, where its points closely approximated the actual values. While RF exhibited competitive performance, SVM proved superior in this context. These results underscore the significance of selecting appropriate ML algorithms tailored to specific machining

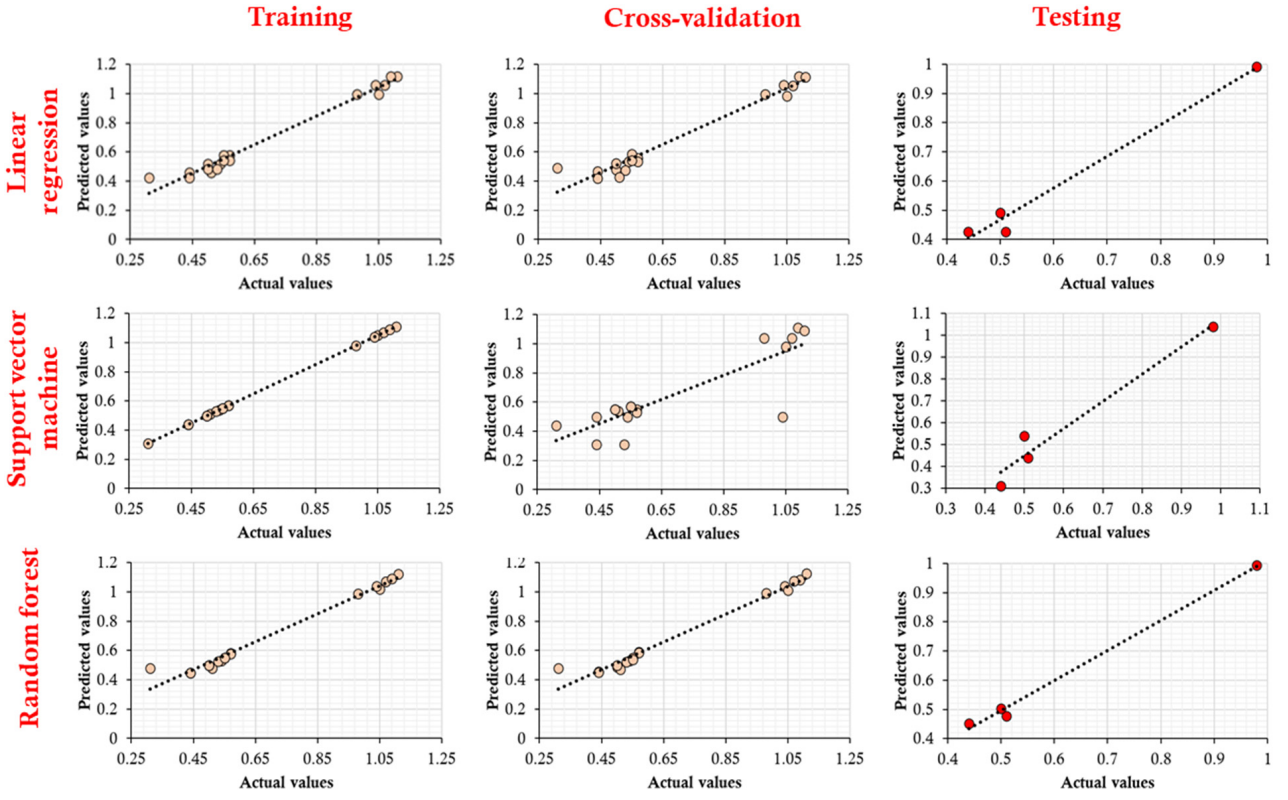

Fig. 10. (Color online) Actual and predicted values of surface roughness under distinct algorithms.

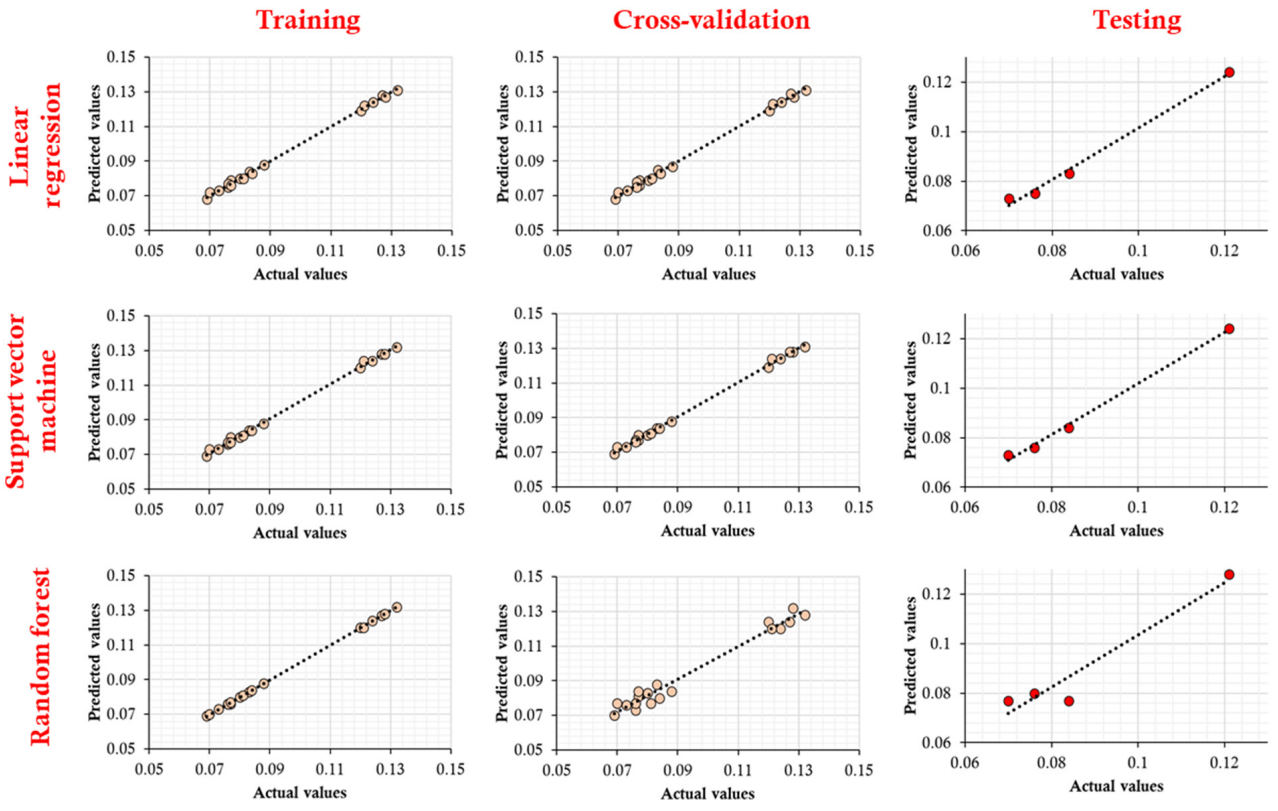

Fig. 11. (Color online) Actual and predicted values of Vb under distinct algorithms.

parameters, emphasizing the necessity of comprehensive training, testing, and cross-validation to ensure precise and robust predictive modeling in manufacturing processes.

6.1. *Quantitative analysis of ML models*

In a regression model, the proportion of variance in the dependent variable (the target) that can be described by the variance in the independent variables (the features) is measured by a statistic called R-squared, which is sometimes referred to as the coefficient of determination.[34]

$$R^2 = 1 - \frac{\text{Sum of Squared Residuals}}{\text{Total Sum of Squares}}.$$

The sum of the squared disparities amid the actual values and the expected values is referred to as the sum of squared residuals. The entire sum of squares represents the total variation in the variable that is being measured.

The average absolute alteration in MAE amid the actual and the expected values is what the MAE metric measures.[35] It treats all errors with the same significance and is less sensitive to extreme values than other methods.

$$\text{MAE} = \frac{1}{n} \times \sum(\text{actual} - \text{predicted}),$$

where n is the number of data points and Σ is the sum of absolute differences for all data points.

RMSE is similar to MAE but takes the square root of the mean of the squared differences, which gives more weight to larger errors.[36]

$$\text{RMSE} = \sqrt{\frac{1}{n} \times \sum(\text{actual} - \text{predicted})^2},$$

where n is the number of data points and Σ is the sum of squared differences for all data points.

RAE measures the relative error amid the actual and expected values by normalizing the MAE using the mean of the actual values.[37] It indicates the error as a proportion of the mean of the actual values.

$$\text{RAE} = \frac{\frac{1}{n} \times \sum(\text{actual} - \text{predicted})}{\frac{1}{n} \times \sum(\text{actual} - \text{mean(actual)})},$$

where mean(actual) is the mean of the actual values.

RRSE is similar to RAE but uses RMSE instead of MAE.[38] It normalizes the RMSE using the standard deviation of the actual values.

$$\text{RRSE} = \sqrt{\frac{\frac{1}{n} \times \sum (\text{actual} - \text{predicted})^2}{\frac{1}{n} \times \sum (\text{actual} - \text{mean}(\text{actual}))^2}}.$$

These are the noteworthy quantitative measures commonly employed in ML. The possibility of metrics hinges on the type of data and the goals of the ML work. It's important to select the most appropriate metrics to evaluate the model's performance effectively. Figure 12 presents the quantitative analysis of distinct algorithms under testing and training.

For Ra, the R^2 produced by RF is 1, MAE is 0.000, RMSE is 0.000, RAE is 0.00% and RRSE is 0.00% for training. RF surpassed other algorithms in terms of training Ra. On the other hand, RF outperformed in testing with the higher R^2 of 0.9969 and lower MAE, RMSE, RAE, and RRSE values. Table 3 presents the quantitative values of R^2, MAE, RMSE, RAE, and RRSE in relation to all algorithms. SVM yields an R^2 of 0.999 for Vb, an MAE of 0.0001, an RMSE of 0.0002, a RAE of 0.53%, and an RRSE of 1.03% for training. SVM trained Vb better than other techniques. However, SVM performed better in testing, as seen by its higher R^2 of 0.9969 and lower values for MAE, RMSE, RAE, and RRSE. The quantitative values of R^2, MAE, RMSE, RAE, and RRSE for each method are displayed in Table 4.

Quantitative analysis of Ra and Vb forecasts was performed using ML algorithms (LR, SVM, and RF)

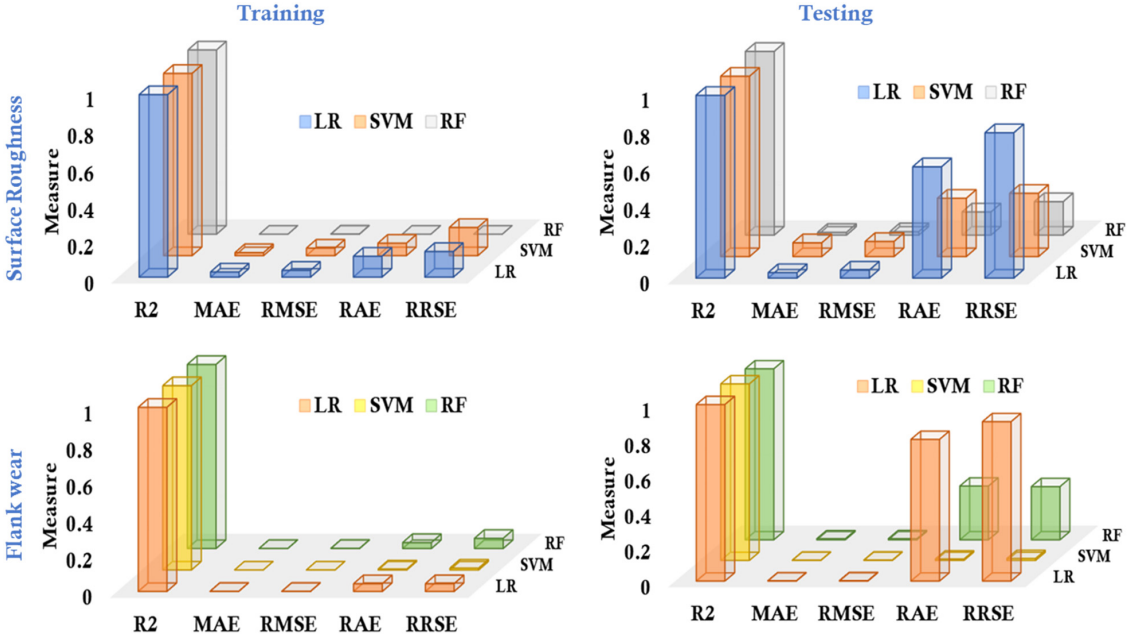

Fig. 12. (Color online) Quantitative analysis of distinct algorithms under testing and training.

Table 3. Quantitative analysis for surface roughness with ML algorithms.

	Training			Testing		
Quantitative analysis	LR	SVM	RF	LR	SVM	RF
R^2	0.9903	0.9891	1.0000	0.9786	0.9912	0.9969
MAE	0.0281	0.0167	0.0000	0.075	0.0298	0.0151
RMSE	0.0375	0.0412	0.0000	0.0822	0.0435	0.0188
RAE	11.36%	6.77%	0.00%	31.67%	12.60%	6.39%
RRSE	13.93%	15.30%	0.00%	34.36%	18.18%	7.87%

Table 4. Quantitative analysis for flank wear with ML algorithms.

	Training			Testing		
Quantitative analysis	LR	SVM	RF	LR	SVM	RF
R^2	0.9991	0.9999	0.9988	0.9912	0.9969	0.9786
MAE	0.0009	0.0001	0.0007	0.0298	0.0151	0.075
RMSE	0.001	0.0002	0.0013	0.0435	0.0188	0.0822
RAE	4.21%	0.53%	3.26%	60.39%	0.12%	31.67%
RRSE	4.23%	1.03%	5.52%	78.86%	0.18%	34.36%

and it was found that different algorithms perform better for each of these two output conditions. Specifically, RF performed better for Ra, while SVM performed better for Vb. This recommends that the choice of algorithm can have a key impact on the predictive performance for different types of data.

7. Classifications based on ML Models

Figure 13 presents the confusion matrix for RF and SVM under distinct environmental conditions. A confusion matrix is a technique that compares measured and predicted results to assess how well the classification model performs. This aids in comprehending the precision and error distribution of the model.[39] In the exploration of Ra, classification analyses using RF and SVM models were conducted for both training and testing phases. During RF-Training, the model exhibited exemplary performance with a perfect classification matrix, accurately assigning six instances for each lubrication condition — dry machining, MQL, and SL-MQL. This emphasized the RF model's robust learning capabilities in comprehensively categorizing Ra values during the training process. Transitioning to RF-Testing, the model demonstrated its predictive accuracy, correctly classifying one instance for dry machining, one for MQL, and two for SL-MQL, showcasing its ability to generalize effectively to unseen testing conditions. Similarly, SVM-Training yielded impeccable classification results, accurately assigning six instances for dry and MQL, and there is a mismatch in the SL-MQL. In SVM-Testing, the model maintained its reliability, correctly categorizing instances for dry machining, SL-MQL, and there is a mismatch in the MQL.

The Vb values obtained during the machining experiments were used for classification analysis using RF and SVM models for both training and testing phases. In RF-Training, the classification matrix revealed accurate categorization, with six instances correctly identified for dry machining, four for MQL, and five for SL-MQL, demonstrating the model's capability to learn from the training dataset. Subsequent RF-Testing demonstrated the model's predictive performance, correctly classifying one instance for dry machining, one for MQL, and one for SL-MQL, indicative of the model's reliability during unseen testing scenarios.

Similarly, SVM-Training displayed perfect classification, correctly categorizing all instances for each lubrication condition, highlighting the robustness of the SVM model in learning the underlying patterns within the training dataset. The SVM-Testing phase further confirmed the model's efficacy, accurately classifying one instance for dry machining and two instances for SL-MQL, reinforcing the reliability of the model in predicting flank wear values under different lubrication conditions. Overall, these classification analyses utilizing RF and SVM models showcase their proficiency in categorizing Ra and Vb values and provide valuable insights into the machining performance under various lubrication conditions

The precision, recall, and F-measure metrics offer a comprehensive evaluation of the classification performance for both the RF and SVM models during training and testing phases. Precision measures the accuracy of the positive predictions made by the model. It is the ratio of true positives to the total predicted positives. Recall reflects the model's ability to correctly identify all actual positive cases. It is the ratio of true positives to the total actual positives. F-measure is the harmonic mean of precision and recall, providing a balanced evaluation when precision and recall are both important. It combines both

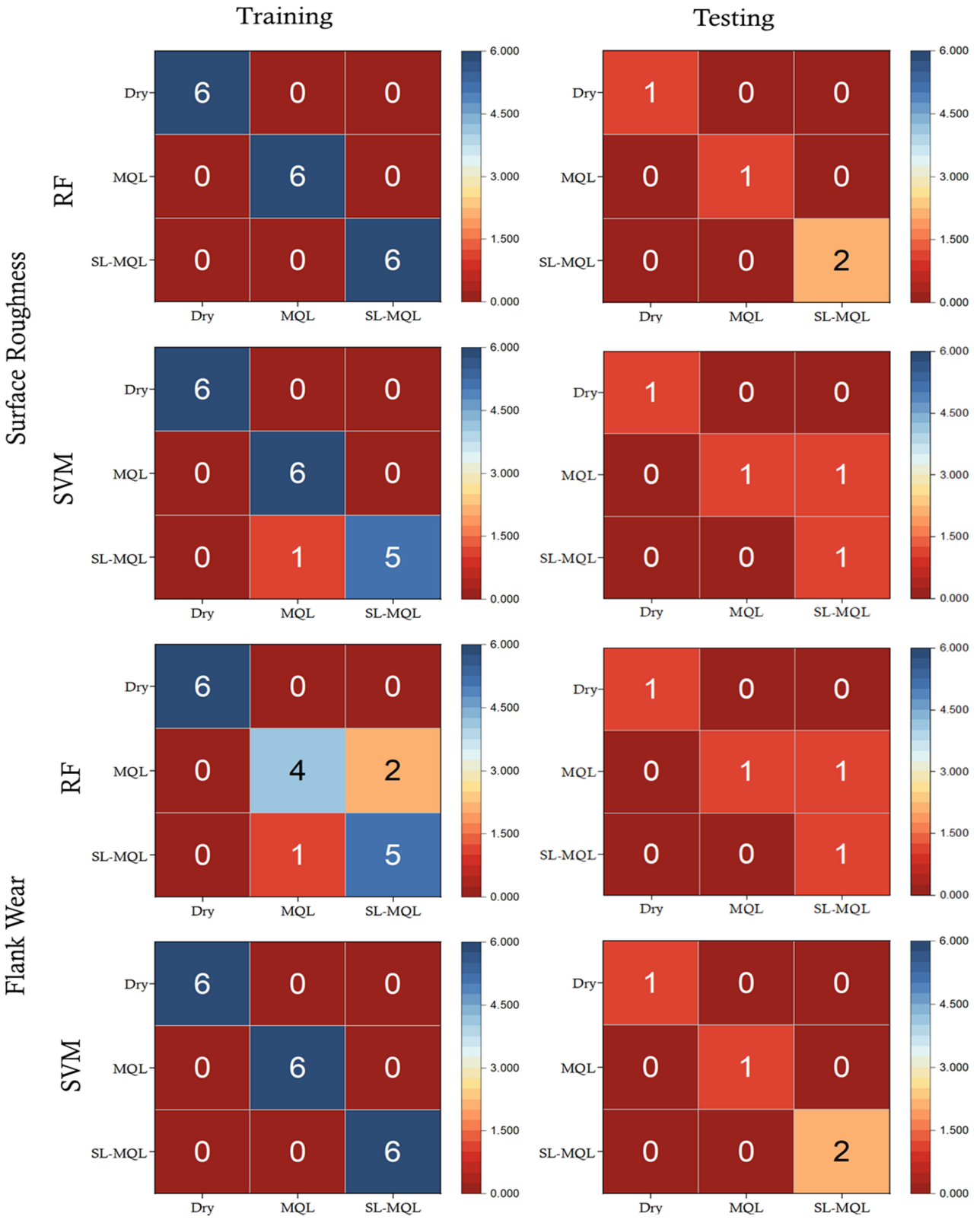

Fig. 13. (Color online) Confusion matrix for RF and SVM models.

metrics into a single score. Tables 5–8 present the classifier values with the distinct algorithms. Figure 14 presents the classification analysis of distinct algorithms under testing and training. In the training sessions of both RF and SVM models, perfect scores of 1 were achieved across all lubrication conditions — dry machining, MQL, and SL-MQL. These results underscore the models' ability to accurately classify instances and maintain a balance between precision and recall. During the testing phase of RF, precision, recall, and *F*-measure remained consistently perfect across all lubrication conditions, emphasizing the model's robust generalization to unseen data. In contrast, the SVM testing phase demonstrated high precision for all lubrication conditions but revealed variations in recall and *F*-measure. Specifically, for MQL and SL-MQL, a slight decrease in recall and *F*-measure values was observed, indicating potential challenges in capturing all relevant instances. In the training phase of the RF model, precision, recall, and *F*-measure demonstrated excellent values of 1 across all lubrication conditions, signifying perfect accuracy in classifying instances for dry machining, MQL, and SL-MQL. In the testing phase of RF, the precision

Table 5. Roughness classifier for RF model.

	Training			Testing		
Environments	Precision	Recall	*F*-Measure	Precision	Recall	*F*-Measure
Dry	1	1	1	1	1	1
MQL	1	1	1	1	1	1
SL-MQL	1	1	1	1	1	1

Table 6. Roughness classifier for SVM model.

	Training			Testing		
Environments	Precision	Recall	*F*-measure	Precision	Recall	*F*-measure
Dry	1	1	1	1	1	1
MQL	0.85	1	0.92	1	0.5	0.667
SL-MQL	1	0.83	0.9	0.5	1	0.667

Table 7. Flank wear classifier for RF model.

	Training			Testing		
Environments	Precision	Recall	*F*-measure	Precision	Recall	*F*-measure
Dry	1	1	1	1	1	1
MQL	0.8	0.6	0.72	1	0.5	0.667
SL-MQL	0.74	0.83	0.76	0.5	1	0.667

Table 8. Flank wear classifier for SVM model.

	Training			Testing		
Environments	Precision	Recall	*F*-measure	Precision	Recall	*F*-measure
Dry	1	1	1	1	1	1
MQL	1	1	1	1	1	1
SL-MQL	1	1	1	1	1	1

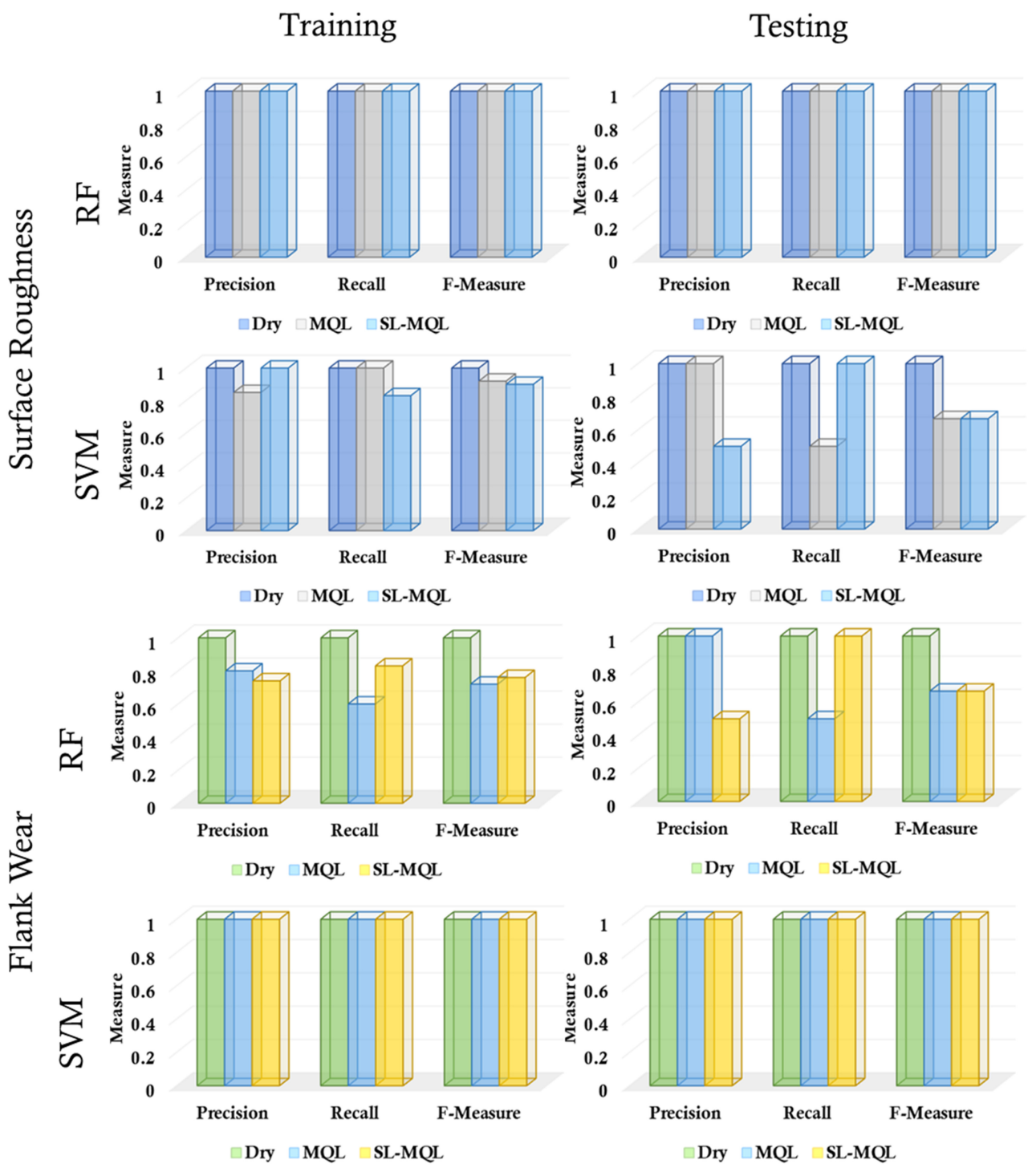

Fig. 14. (Color online) Classification analysis of distinct algorithms under testing and training.

values for MQL and SL-MQL remained high, but the recall values indicated a potential underestimation of instances, resulting in slightly lower *F*-measure values. Moving to the SVM model, both training and testing phases showcased impeccable classification performance. Precision, recall, and *F*-measure all yielded perfect scores of 1 across dry machining, MQL, and SL-MQL in both phases. These results

suggest the SVM model's ability to classify instances consistently and accurately under various lubrication conditions, highlighting its robustness in capturing relevant information during both training and testing scenarios. Overall, the utilization of precision, recall, and *F*-measure metrics provided a comprehensive and nuanced evaluation of the classification models, offering insights into their performance in discerning surface roughness values under different lubrication conditions.

8. Conclusions

Under this study, Mg-AZ91D is milled with SL-MQL, MQL, and dry conditions. It is determined that the milling input parameters, environmental factors, and output parameters are related to one another. To forecast the output of milling parameters, several ML training models are tested using the experimental data.

- In comparison to dry cutting, the Ra significantly dropped under MQL and SL-MQL milling conditions. The Ra achieved under SL-MQL conditions is 8–13% lower than that obtained under MQL cutting technique and 49–70% lower than that obtained under dry conditions. Under the dry cutting approach, SEM images of the machined face reveal more scratches and uneven feed marks. On the other hand, SL-MQL generates smooth surfaces, which in turn reflect under 3D surface topography with fewer peaks and valleys.
- The Vb dropped considerably during MQL and SL-MQL milling conditions compared to dry cutting. The decrease in cutting temperature is the cause of the phenomenon. The Vb attained under SL-MQL circumstances is 8–11% lower than that under MQL settings and 41–54% lower than that under dry cutting method. SEM images revealed that wear is reduced under SL-MQL with less coating delamination.
- When it came to surface finish forecasting, the RF algorithm topped out SVM and linear regression among the ML algorithms under consideration. SVM, however, showed comparatively superior outcomes than other models used in this study when it came to Vb prediction.
- The RF and SVM models demonstrated strong classification performance in accurately categorizing Ra and Vb values across diverse lubrication conditions. Both models exhibited excellent precision, recall, and *F*-measure scores during training and testing, showcasing their robust learning capabilities.

Acknowledgment

The authors express appreciation to the Abdul Hakeem College of Engineering & Technology, for supporting this study.

Authors' Contribution

Amjath Z A: Data curation, formal analysis, investigation, methodology, project administration, and supervision. **Ganesa Moorthy R:** Formal analysis, investigation, and methodology, **Ashraff Ali K S:** Formal analysis, Investigation, methodology, and project administration. **C. Gnanavel:** Formal analysis, Investigation.

Funding

Not applicable

Data Availability

Not applicable

Conflict of Interest

The authors declare no competing interests.

References

1. R. Saravanan *et al.*, *Rev. Adv. Mater. Sci.* **62** (2023) 1.
2. A. Alshibi, A. Nasreldin and S. Pervaiz, *Lubricants* **11** (2023) 079, doi: 10.3390/lubricants11020079.
3. M. S. Zakaria *et al.*, *J. Mater. Res. Technol.* **19** (2022) 3685, doi: 10.1016/j.jmrt.2022.06.127.
4. N. Khanna and P. Shah, *Energy Efficiency Analysis for Machining Magnesium Metal Matrix Composites Using In-house Developed Hybrid Machining Facilities* (Springer International Publishing, 2020).
5. K. Nimel Sworna Ross and G. Manimaran, *J. Brazilian Soc. Mech. Sci. Eng.* **41** (2019) 44, doi: 10.1007/s40430-018-1552-3.
6. M. Jamil *et al.*, *Appl. Therm. Eng.* **177** (2020) 115480, doi: 10.1016/j.applthermaleng.2020.115480.

7. L. Li *et al.*, *J. Mater. Res. Technol.* **27** (2023) 1665, doi: 10.1016/j.jmrt.2023.10.003.
8. J. Xu *et al.*, *J. Mater. Res. Technol.* **26** (2023) 9380, doi: 10.1016/j.jmrt.2023.09.209.
9. R. Vishal, K. Nimel Sworna Ross, G. Manimaran and B. K. Gnanavel, *Mater. Perform. Charact.* **8** (2019) 527, doi: 10.1520/MPC20190154.
10. C. P. Khunt, M. A. Makhesana, K. M. Patel and B. K. Mawandiya, *Mater. Today Proc.* **44** (2021) 341, doi: 10.1016/j.matpr.2020.09.741.
11. N. S. Ross, P. T. Sheeba, M. Jebaraj and H. Stephen, *Mater. Manuf. Process.* **37** (2022) 327, doi: 10.1080/10426914.2021.2001510.
12. C. Darshan *et al.*, *Int. J. Adv. Manuf. Technol.* **105** (2019) 1851, doi: 10.1007/s00170-019-04544-x.
13. M. A. Makhesana and K. M. Patel, *Adv. Mater. Process. Technol.* **8** (2022) 2102, doi: 10.1080/2374068X.2021.1882123.
14. N. S. Ross *et al.*, *J. Intell. Manuf.* **35** (2024) 757, doi: 10.1007/s10845-023-02074-8.
15. G. S. Prashanth, P. Sekar, S. Bontha and A. S. S. Balan, *Mater. Manuf. Process.* **38** (2023) 235, doi: 10.1080/10426914.2022.2116043.
16. M. P. Motta *et al.*, *Procedia CIRP* **108** (2022) 710, doi: 10.1016/j.procir.2022.03.110.
17. M. Brillinger, M. Wuwer, M. Abdul Hadi and F. Haas, *CIRP J. Manuf. Sci. Technol.* **35** (2021) 715, doi: 10.1016/j.cirpj.2021.07.014.
18. V. Velmurugan, G. Manimaran and K. N. S. Ross, *J. Brazilian Soc. Mech. Sci. Eng.* **43** (2021) 380, doi: 10.1007/s40430-021-03098-y.
19. L. D. K. Catherine and D. A. Hamid, *IOP Conf. Ser. Mater. Sci. Eng.* **1062** (2021) 012054, doi: 10.1088/1757-899X/1062/1/012054.
20. K. N. S. Ross and G. Manimaran, *Arab. J. Sci. Eng.* **45** (2020) 9267, doi: 10.1007/s13369-020-04728-8.
21. Z. W. Zhong, *Mater. Manuf. Process.* **36** (2021) 987.
22. N. S. Ross *et al.*, *J. Mater. Res. Technol.* **31** (2024) 1837, doi: 10.1016/j.jmrt.2024.06.183.
23. M. E. Korkmaz, M. K. Gupta, N. S. Ross and V. Sivalingam, *Sustain. Mater. Technol.* **36** (2023) e00641, doi: 10.1016/j.susmat.2023.e00641.
24. C. Divya, L. Suvarna Raju and B. Singaravel, *Mater. Manuf. Process.* **36** (2021) 1781, doi: 10.1080/10426914.2021.1945097.
25. S. Dinesh, V. Senthilkumar, P. Asokan and D. Arulkirubakaran, *Mater. Des.* **87** (2015) 1030, doi: 10.1016/j.matdes.2015.08.099.
26. K. N. SwornaRoss and R. M. Ganesh, *J. Fail. Anal. Prev.* **19** (2019) 821, doi: 10.1007/s11668-019-00667-1.
27. G. Manimaran and K. Nimel Sworna Ross, *J. Test. Eval.* **48** (2020) 3269, doi: 10.1520/JTE20180130.
28. N. S. Ross, K. N. S. Ross and G. Manimaran, *J. Brazilian Soc. Mech. Sci. Eng.* **41** (2019) 44, doi: 10.1007/s40430-018-1552-3.
29. D. Y. Pimenov *et al.*, *J. Mater. Res. Technol.* **11** (2021) 719, doi: 10.1016/j.jmrt.2021.01.031.
30. R. Guha, A. Suresh, J. DeFrain and K. Deb, *Mater. Manuf. Process.* **38** (2023) 1997, doi: 10.1080/10426914.2023.2220487.
31. P. Pathak and P. Choudhary, A comprehensive review of various machine learning techniques, in *Explainable Machine Learning Models and Architectures* (2023), pp. 1–10, doi: 10.1002/9781394186570.ch1.
32. A. Dhilip, J. Nampoothiri, M. Senthilkumar and N. Kirubanandan, *Mater. Manuf. Process.* **38** (2022) 1650, doi: 10.1080/10426914.2022.2146713.
33. S. S. Nain, D. Garg and S. Kumar, *Mater. Manuf. Process.* **33** (2018) 1793, doi: 10.1080/10426914.2018.1476761.
34. M. E. Korkmaz *et al.*, *J. Mater. Res. Technol.* **27** (2023) 4074, doi: 10.1016/j.jmrt.2023.10.192.
35. V. H. Nguyen *et al.*, *Math. Probl. Eng.* **2021** (2021) 6815802, doi: 10.1155/2021/6815802.
36. J. Ni *et al.*, *J. Clean. Prod.* **320** (2021) 128888, doi: 10.1016/j.jclepro.2021.128888.
37. M. Kumar *et al.*, *Measurement* **224** (2024) 113937, doi: 10.1016/j.measurement.2023.113937.
38. W. K. Adu, P. Appiahene and S. Afrifa, *J. Electr. Syst. Inf. Technol.* **10** (2023) 12, doi: 10.1186/s43067-023-00078-1.
39. M. Danish *et al.*, *Results Eng.* **22** (2024) 102015, doi: 10.1016/j.rineng.2024.102015.